International Journal of Biological Macromolecules 242 (2023) 125000

Contents lists available at ScienceDirect

International Journal of Biological Macromolecules

journal homepage: www.elsevier.com/locate/ijbiomac

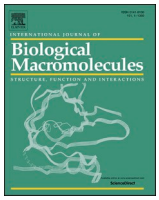

Formulation development of collagen/chitosan-based porous scaffolds for skin wounds repair and regeneration

Caterina Valentino [a], Barbara Vigani [a], Gaia Zucca [a], Marco Ruggeri [a], Cinzia Boselli [a], Antonia Icaro Cornaglia [b], Lorenzo Malavasi [c], Giuseppina Sandri [a], Silvia Rossi [a,*]

[a] Department of Drug Sciences, University of Pavia, Viale Taramelli 12, 27100 Pavia, Italy
[b] Department of Public Health, Experimental and Forensic Medicine, University of Pavia, via Forlanini 2, 27100 Pavia, Italy
[c] Department of Chemistry and INSTM, University of Pavia, Viale Taramelli 16, 27100 Pavia, Italy

ARTICLE INFO

Keywords:
Collagen
Chitosan
Wound healing
Cross-linking
DoE approach

ABSTRACT

Herein we developed a hydrogel based porous cross-linked scaffold intended for the treatment of chronic skin ulcers. It is made of collagen, the most abundant protein of mammals ECM, and chitosan, a natural polysaccharide endowed with numerous positive cues for wound repair. Different cross-linking methods, namely UV irradiation with the addition of glucose, addition of tannic acid as cross-linking agent and ultrasonication, were employed to prepare a cross-linked hydrogel with a highly interconnected 3D internal structure. The variables considered critical to obtain a suitable system for the envisaged application are the composition of hydrogels, especially the concentration of chitosan, and the concentration ratio between chitosan and collagen. Stable systems, characterized by high porosity, were obtained thanks to the use of freeze-drying process. To assess the influence of the above-mentioned variables on scaffold mechanical properties, a Design of Experiments (DoE) approach was exploited, which resulted in the identification of the best hydrogel composition. In vitro and in vivo assays on a fibroblast model cell line and on a murine model, respectively, demonstrated scaffold biocompatibility, biomimicry, and safety.

1. Introduction

Chronic injuries represent a public health problem that affects 40 million people worldwide, reaching epidemic proportions, with a huge impact on the economy of several countries. Generally, chronic wounds are characterized by persistent inflammation, difficulty in re-epithelization and angiogenesis processes. The causes are attributable to age, persistent injuries or pathological conditions (e.g. diabetes mellitus, malignant tumors, obesity, cardiovascular disease), but also to an inadequate treatment of the primary wound [1,2].

Skin wounds, in particular chronic ones, are characterized by a process of non-recovery that makes the application of medications essential to promote and facilitate the restoration of the physiological conditions and the integrity of the skin barrier [3,4]. Modern wound dressings represent an evolution of traditional systems (cotton wool, natural or synthetic bandages, gauzes, and patches) for the treatment of skin wounds [5–7]. These dressings not only cover the lesion, but also promote the healing process, creating a moist environment and interacting with endogenous substances present at the site of damage [8,9]. Among modern dressings, hydrogels have gained an increasing attention during recent years [10]. Hydrogels are semi-solid, three-dimensional natural or synthetic polymeric networks, where water represents the liquid component. Because of their hydrophilic properties and internal 3D structure, they could swell reversibly and absorb relevant amounts of water or biological fluids, thus helping the diffusion of nutrients [11]. Thanks to their mechanical stiffness and biochemical and topological cues in promoting cell physiological functions, hydrogels are recognized to be able to mimic the extracellular matrix (ECM), and thus to promote cell proliferation and migration. In addition, their porous structure makes them suitable for cellular processes and guarantees the release of nutrients and growth factors [12,13].

The use of natural polymers in tissue engineering has reached great interest compared to synthetic polymers, due to specific physicochemical and biological properties, including biocompatibility and adequate biodegradability, low immunogenicity and antigenicity, superior structural design and three-dimensional geometry [14,15]. Furthermore,

* Corresponding author.
E-mail address: silvia.rossi@unipv.it (S. Rossi).

https://doi.org/10.1016/j.ijbiomac.2023.125000
Received 10 February 2023; Received in revised form 18 May 2023; Accepted 19 May 2023
Available online 20 May 2023

natural polymers possess intrinsically natural cell adhesion site, which represents an advantage for cell attachment [11]. However, they show several limitations such as poor reproducibility (related to batch-to-batch variation), scarce processability, and limited availability [16–18]. The natural polymers employed in wound dressings can have different origins: they can derive from ECM (collagen and gelatin), from algae (alginate), from crustaceans (chitosan), or from insects (fibroin and silk sericin) [19].

The most abundant protein in mammals is collagen (Coll), which is known to be the main component of ECM. While providing structure, protection, and support to human tissues, collagen is a relatively simple protein, whose chains are generally formed mainly by three basic amino acids, glycine, proline and hydroxyproline [19,20]. The use of Coll in tissue engineering was extensively investigated, due to its natural abundance, biocompatibility and biodegradability, good permeability, and low immunogenic response. It is recognized as an optimal candidate for tissue engineering scaffolding strategies, including tubes, freeze-dried sponge-like scaffolds, and hydrogels [20,21].

Chitosan (Cs) is a natural polysaccharide derived from the deacetylation of chitin, mainly obtained from the exoskeleton of crustaceans, insects, and fungal cell walls. Cs bioactive properties, including antimicrobial, wound-healing and hemostatic properties, make it attractive for tissue engineering (cartilage, bone, skin, tissue fixation, blood vessel) [22–25].

The main disadvantage of natural-based scaffolds is related to their poor mechanical properties (stiffness and brittleness), which cause low mechanical resistance [26]. The use of cross-linking strategies leads to the formation of a 3D network which, in turn, allows to obtain scaffolds with suitable mechanical properties, compared to the target tissue or organ [27,28]. According to the literature, freeze-drying is a successful technique to prepare dried hydrogels for wound healing. This approach provides sponge-like systems characterized by porosity and surface properties functional to wound healing [11,28,29]. Moreover, these systems can be loaded with therapeutic agents, such as growth factors and antibiotics [20].

The present work aims to develop a porous cross-linked scaffold based on Coll and Cs intended for skin repair and regeneration. Different cross-linking methods have been investigated: UV irradiation in presence or in absence of glucose, treatment with tannic acid, and ultrasonication. In particular, the focus of the present work is to compare the physicochemical and biopharmaceutical properties of Coll and Cs- based scaffolds obtained with the three different above-mentioned cross-linking methods to evaluate the most effective system for the envisaged application. To the best of our knowledge, to date, such a comparison was not investigated. Beside the cross-linking method, the variables that have been considered critical concern the composition of hydrogels, especially the concentration of Cs and the Cs/Coll weight ratio. To assess the influence of these variables on scaffold mechanical properties, a Design of Experiments (DoE) approach was exploited.

2. Materials and methods

2.1. Materials

Chitosan (Cs), deacetylation grade >75 %, medium molecular weight (190 kDa-310 kDa), D-(+)-Glucose (GLUC) and Tannic acid (TA) MW 1701,20 g/mol, were purchased from Sigma-Aldrich (Italy); Native animal collagen soluble 1 % *w/v* from Kelisema (Italy).

2.2. Methods

2.2.1. Hydrogels preparation

Medium molecular weight Cs was dissolved at 2 % *w*/w in 0.5 M acetic acid under magnetic stirring at room temperature (RT). The solution was then centrifuged at 8000 rpm for 10 min at 20 °C to remove undissolved impurities naturally present in Cs powder. Coll 1 % *w/v* solution was dialyzed against deionized water with a dialysis membrane (12,000–14,000 Da) at 4 °C for 24 h, changing the water every hour, in order to remove the preservatives, present in the commercial solution. After 24 h Coll was frozen at −20 °C and then subjected to sublimation for 48 h using Heto DRYWINNER (Analitica De Mori, Milan, I). Freeze-dried Coll was then dissolved at 2 % *w*/w in MilliQ water under bland magnetic stirring. Both Cs and Coll solutions were prepared at RT and maintained under stirring overnight. Afterwards, they were mixed at 1:1 weight ratio.

Different cross-linking methods were considered and investigated in order to enhance the interaction between the two components.

2.2.1.1. Glucose (GLUC) and UV irradiation. Coll/Cs mixture was put in a 6-well plate and placed under UV irradiation (λ = 254 nm) for 30 min. Such time was selected to have a cross-linking effect without protein denaturation [30]. In order to enhance the efficiency of UV cross-linking, GLUC was added to the solution at a protein/GLUC ratio equal to 4.65 (*w*/w).

2.2.1.2. Tannic acid (TA). TA was selected since it can establish hydrogen bonds with the amino and amide-residues of Coll and Cs molecules [31]. TA powder was dissolved at 10 % w/w, calculated as percentage of the total amount of polymers (Coll + Cs), in MilliQ water, under magnetic stirring and at RT. TA solution was then added at 1:1 ratio to Coll/Cs solution under magnetic stirring, until homogeneous violet coloring was reached, indicating that the cross-linking was occurred.

2.2.1.3. Ultrasonication (US). Coll/Cs mixture was placed into an ultrasonicator Elmasonic S 80 H (Elma Schmidbauer GmbH, Germany) at a temperature ranging into the interval 35–40 °C for 30 min. After that, the gelation process was completed leaving the solutions for 24 h at RT [32].

2.2.2. Hydrogels rheological characterization

All the Coll/Cs mixtures upon cross-linking were subjected to viscosity measurements by means of a rotational rheometer (MCR 102, Anton Paar, Turin, Italy) equipped with a cone plate combination (CP25, diameter = 25 mm; angle = 1°) as measuring system. Viscosity was measured at 25 °C by applying increasing shear rates (10–600 s^{-1}) and setting a gap of 0.101 mm. Pristine Coll and Cs solutions, as well as their mixture not subjected to cross-linking methods, were used as references. Three replicates were performed for each sample. Viscosity variation % ($\frac{\eta_{mix}}{\eta_t}$ %) was calculated according to the equation reported later in the text to evaluate the change in viscosity due to the interaction between the two polymers involved.

$$\frac{\eta_{mix}}{\eta_t}\% = \frac{\eta\,(Coll/Cs)}{\eta(Coll) + \eta(Cs)} \times 100$$

where:

- $\eta\,(Coll/Cs)$ = viscosity of the Coll/Cs mixture (as such or after cross-linking);
- $\eta(Coll) + \eta(Cs) = \eta_t$ = theoretical value calculated as the sum of the viscosities of Coll and Cs solutions at the same concentrations as in the mixture.

2.2.3. Freeze-dried hydrogels preparation

Cross-linked Coll/Cs mixtures (hydrogels) were placed in a 24-well plate (2.5 mL/well) and subjected to freezing at −20 °C for 24 h and then to sublimation for 48 h (Heto DRYWINNER).

Table I
Quali-quantitative composition of Coll/Cs hydrogels expressed as % *w*/w and scheme of full factorial design 3^2.

US freeze-dried hydrogels	[Cs] % w/w	[Cs]/[Coll]	[Coll] % w/w	[Cs]	[Cs]/[Coll]
Coll/Cs 1	0.5	2	0.25	−1	+1
Coll/Cs 2	0.5	1	0.5	−1	0
Coll/Cs 3	0.5	0.5	1	−1	−1
Coll/Cs 4	0.75	2	0.375	0	+1
Coll/Cs 5	0.75	1	0.75	0	0
Coll/Cs 6	0.75	0.5	1.5	0	−1
Coll/Cs 7	1	2	0.5	+1	+1
Coll/Cs 8	1	1	1	+1	0
Coll/Cs 9	1	0.5	2	+1	-1

2.2.4. Freeze-dried hydrogel characterization

2.2.4.1. Morphological analysis. Morphological evaluation of each freeze-dried hydrogel was performed by Scanning Electron Microscope (SEM) Mira3 XMU (Tescan, Brno-Kohoutovice, Czech Republic). Samples were mounted on a steel stub and made conductive by graphite deposition under vacuum (sputtering). Images were obtained at high voltage, in high vacuum, at room temperature and at different magnifications.

Pore size dimensional analysis was calculated using the imaging analysis program ImageJTM 2.0 (net.imagej: imagej:2.0.0-rc-55, Java-based operating system, 2009, National Institutes of Health, Bethesda, MD, USA).

2.2.4.2. FTIR analysis. Infrared spectra were collected by a PerkinElmer Spectrum 100 Fourier transform infrared (FT-IR) spectrometer in the attenuated total reflectance (ATR) mode (PerkinElmer, Waltham, MA, USA). Cs 1 % *w*/w, Coll 1 % w/w and Coll/Cs 1 % w/w mixture upon freeze-drying were used. Three spectra for each sample were collected to obtain an average spectrum.

2.2.4.3. Hydration properties assessment. Hydration properties of the freeze-dried scaffolds were measured by soaking samples previously weighed (≈50 mg) into 20 mL of PBS 10 % at pH 7.4 for 24 h at 37 °C. Then, each sample was blandly dabbed to remove excess PBS and weighted. Each experiment was carried out in triplicate. The amount of PBS absorbed was calculated at each time selected (30 min, 1 h, 3 h, 6 h, 24 h) as follows:

$$amount\ of\ PBS\ absorbed\ (g) = W_f - W_i$$

Swelling ratio, defined as the fractional increase in weight of the hydrogel upon water absorption, was calculated at 24 h as follows:

$$S = \frac{W_f - W_i}{W_i} \times 100$$

where:

S = swelling ratio;
W_f = weight of the hydrated scaffold;
W_i = weight of the dried scaffold.

2.2.4.4. Mechanical properties assessment. Freeze-dried hydrogels, as such and upon hydration in PBS for 24 h at 37 °C, were subjected to a compression test by means of TA.XT plus Texture Analyzer (Stable Micro System, Godalming, UK) equipped with a 5 kg load cell. For the analysis, probe P/0.25 S was lowered into the sample at a constant speed of 0.5 mm/s to a final distance equal to 70 % of the sample height; afterwards the probe was raised with a constant speed of 5.0 mm/s. For both dried and hydrated samples three replicates were performed. Compression stress (Pa) vs strain profiles were recorded for each sample. Work of compression was also calculated as the area under the curve force vs displacement (AUC, N·*mm*).

Hydrated samples were also subjected to dynamic oscillatory measurements at 37 °C by means of a rotational rheometer (MCR102, Anton Paar, Turin, Italy), using a parallel plate combination (PP25, diameter = 25 mm) as measuring system. A stress sweep test was performed at a constant frequency (1 Hz) and the elastic response of the sample, expressed as storage modulus G′, was measured as a function of stress; such a test allowed the identification of the linear viscoelastic region, characterized by constant G′ values on increasing stress. Then, samples were subjected to oscillation test: a shear stress chosen in the linear viscoelastic region previously determined, was applied at increasing frequencies (1–20 Hz) and G′ (storage modulus) and G″ (loss modulus) values were recorded as a function of frequency. Loss tangent (tg δ) parameter was calculated as the ratio between G″ (loss modulus) and G′ (storage modulus) at frequency values of 1, 5 and 10 Hz. Three replicates were considered for each sample.

2.2.5. Design of Experiments (DoE) approach

In the case of Coll/Cs hydrogels cross-linked by US (US freeze-dried hydrogels), different Cs and Cs/Coll weight ratios were investigated.

A DoE approach was employed in order to evaluate, on a statistical basis, the contribution of different parameters on the mechanical properties of the freeze-dried hydrogels. A “full factorial design” containing all possible combinations between the factors and their levels was chosen. Table I reports the quali-quantitative composition of Coll/Cs ultrasonicated (US) freeze-dried hydrogels together with the scheme of the 3^2 full factorial design.

In particular, 2 factors, namely Cs concentration (% *w*/w) and Cs/Coll weight ratio, were investigated at three levels, high (+), medium (0) and low (−): Cs concentration ([Cs]) (%w/w): 0.5 % (−); 0.75 % (0); 1 % (+); Cs/Coll weight ratio ([Cs]/[Coll]) (%w/w): 0.5 % (−); 1 % (0); 2 % (+).

Maximum compression stress (Stress, Pa) and work of compression (AUC, N·mm), of freeze-dried hydrogels as such and upon hydration in PBS were measured as reported in Section 2.2.4.4 and considered as the response variables. Chemometric Agile Tool software was used to generate the model.

2.2.6. US freeze-dried hydrogels characterization

The US freeze-dried hydrogel Coll/Cs 3, 6 and 9 were characterized for morphology, porosity, biodegradation, in vitro cell proliferation and adhesion, and in vivo wound healing properties on an animal model (rat).

2.2.6.1. Morphology analysis. Morphological evaluation of US freeze-dried hydrogels (Coll/Cs 3, 6 and 9) was performed as described in Section 2.2.4.1.

2.2.6.2. Porosity analisys. Porosity of US freeze-dried hydrogels (Coll/Cs 3, 6 and 9) was measured using the liquid displacement method, as reported by Zeng [33]. Briefly, absolute ethanol was used as the displacement liquid, since it can penetrate the porous network without inducing scaffold morphology variation like shrinkage or swelling, being it a Cs non-solvent. Samples (dry mass M_0) were immersed for 1 h in a known volume (10 mL) of absolute ethanol. The procedure was carried out by measuring the whole system weight (sample + ethanol) (M_a). After 1 h, the sample was removed, and the remaining ethanol, not entrapped within the sample pores, was weighted (M_b). At the same time, a calibrated cylinder with a known volume of ethanol (10 mL) was also measured (M_1). Subsequently, the calibrated container was emptied, and the wet sample previously soaked in ethanol for 1 h was placed inside. The ethanol in which has been immersed the scaffold, was then added until the container was filled to the same above-mentioned volume. Lastly, the container was weighted again (M_2). Porosity of the

scaffold (P %) was calculated according to the following equation:

$$P\% = \frac{M_a - M_b - M_0}{(M_a - M_b) - (M_2 - M_1)} \times 100$$

2.2.6.3. Hydration properties assessment. Hydration properties of the US freeze-dried hydrogels (Coll/Cs 3, 6 and 9) were measured as described in Section 2.2.4.3.

2.2.6.4. In vitro degradation test. A degradation test was performed on UC freeze-dried hydrogels (Coll/Cs 3, 6 and 9), in order to evaluate the effectiveness of the crosslinking method. Phosphate buffered saline (PBS) at 10 % *v*/v was used as degradation medium. US freeze-dried hydrogels were placed in Eppendorf tubes, 5 mL of the degradation medium was added to the tubes, and the test was carried out at 37 °C in a thermostatic oscillating water bath. At each time point (t0 = 0 days; t1 = 7 days; t2 = 14 days; t3 = 28 days), hydrated samples were subjected to freezing at −20 °C for 24 h and then to sublimation for 48 h using Heto DRYWINNER. Each experiment was carried out in triplicate. % loss on dry weight due to degradation in PBS was calculated at each time point as follows:

$$W\% = \frac{W_f}{W_i} \times 100$$

where:

W % = % loss on dry weight;
W_i = weight of dry freeze-dried hydrogels, before soaking;
W_f = weight of dry freeze-dried hydrogels at each time point.

Morphological characterization (SEM and dimensional analysis) of each sample at each time point was carried out as described in Section 2.2.4.

2.2.6.5. In vitro adhesion and proliferation test on fibroblast cell line. The proliferation and adhesion properties of US freeze-dried hydrogels (Coll/Cs 3, 6 and 9) have been assessed on normal human dermal fibroblasts (NHDF), from juvenile foreskin (PromoCell, WVR, Milan, Italy). NHDF (2nd-5th passages) were cultured in polystyrene flasks in complete medium (CM), namely Dulbecco's Modified Eagle's Medium (DMEM, Merk Life Science S.r.l., Milan, I), supplemented with 10 % *v*/v heat-inactivated Foetal Bovine Serum (FBS) (VWR International S.r.l, Milan, I), and with 1 % v/v antibiotic-antimycotic solution (Merk Life Science S.r.l., Milan, Italy). Cells were kept incubated at 37 °C in 5 % CO_2 atmosphere. US freeze-dried hydrogels (Coll/Cs 3, 6 and 9) were treated with ethanol, washed with PBS and then exposed to UV-irradiation for 20 min. After sterilization and conditioning with CM, samples with the same size of the well were placed in the apical chamber of a 24-well Transwell® Permeable Support (Corning Incorporated, Corning, New York, USA) and cells were seeded above them at a density of 12,500 cells/cm^2. CM was added to the basolateral chamber to avoid evaporation and samples and cells dryness. Both apical and basolateral medium was changed with fresh CM every 2 days. Cells-sample contact was carried out in the incubator for 3 and 7 days. Four replicates were performed for each sample; CM was used as reference. At days 3 and 7 of culture an Alamar blue assay was performed. In detail, the medium was removed and 250 μL of a 10 % *v*/v solution of Alamar blue in DMEM was added to each well and left in contact for 3 h. After 3 h fluorescence was detected by means of a multi-mode microplate reader (FLUOstar Omega Microplate Reader, BMG LabTech, Ortenberg, G) at two different wavelengths: at 570 nm to detect the reduced form (red) of the Alamar Blue, and 655 nm, to detect the oxidized one (blue). Furthermore, cell adhesion and distribution into US freeze-dried hydrogels (Coll/Cs 3, 6 and 9) at 3 days and 7 days of culture was appreciated by means of confocal laser scanning microscopy (CLSM, Leica TCS SP2, Leica Microsystems, Milan, I). After medium removal, each well was rinsed with PBS and then the cells adhered on the freeze-dried samples were fixed with 3 % *v*/v glutaraldehyde solution in PBS for 1 h, at 8 °C. Afterwards, cells walls were permeabilized with 250 μL of Triton X-100 in PBS for 5 min and, then, cellular cytoskeletons were stained by incubation with 250 μL of tetramethylrhodamine (TRITC) at 20 μg/mL in PBS for 45 min, at RT. Afterwards, each well was washed twice with PBS and cell nuclei were stained with 250 μL of bisbenzimide H334342 trihydrochloride (HOECHST) 1 mg/mL diluted 1:10,000 in PBS for 10 min, at room temperature. Finally, the samples were mounted on a microscope slide, covered using coverslips and analyzed with λ_{ex} = 350 nm and λ_{em} = 470 nm for HOECHST and λ_{ex} = 514 nm and λ_{em} = 580 nm for TRITC. The acquired images were processed with the software associated with the microscope (Leica Microsystem, Milan, Italy).

2.2.6.6. In vivo experiments on murine model. All animal experiments were carried out in full compliance with the standard international ethical guidelines (European Communities Council Directive 2010/63/EU) approved by Italian Health Ministry (D.L. 116/92). The protocol followed was approved by the Local Institutional Ethics Committee of the University of Pavia for the use of animals and by ISS (Istituto Superiore di Sanità). In detail, four male rats (Wistar 200–250 g, Envigo RMS S.r.l.) were subjected to anesthetic treatment with equitensine at 3 mL/kg (39 mM pentobarbital, 256 mM chloral hydrate, 86 mM MgSO4, 10 % *v*/v ethanol, and 39.6 % v/v propylene glycol) and their back was shaved to remove all hair. All animals were then carefully monitored for the following 3 days by animal care services and received additional treatment of the same pharmacological treatments. The preparation of US freeze-dried hydrogels Coll/Cs 3, 6 and 9 was carried out under laminar flow hood. Samples were then cut with a biopsy punch to have a diameter of 4 mm and sterilized through UV irradiation for 24 h, before their usage. Three circular full thickness burns, 4 mm in diameter, were produced on the back of the animals by means of the contact with an aluminum rod (105 °C for 40 s). 24 h later, the formed blisters were removed using a 4 mm diameter biopsy punch to obtain full-thickness lesions. 4 mm diameter sample previously prepared were applied on the lesions. Lesions treated with 20 μL of saline solution were the negative control. Lesions were covered with a sterile gauze and the rat back was wrapped with a surgery stretch (Safety, Italy) to protect lesions. 18 days after the treatment, full thickness biopsies were taken in correspondence of the initial lesions and the histological analysis of the excised tissues was performed. A biopsy of intact skin was also taken for comparison. Hematoxylin and eosin (H&E) were used to stain some sections, while picrosirius red (PSR) was used on others. Following deparaffinization, the sections were hydrated, lightly stained with Weigert's hematoxylin to identify the nuclei, and then stained with PSR (1 h). Following that, after dehydration, xylene was used to clean each section, which was then mounted with DPX mounting medium. Stained sections were observed with a light microscope Carl Zeiss Axiophot provided, for circular polarizing microscopy, with suitable filters in the condenser stage and in the microscope tube. A microscope digital 5 megapixels CCD camera Nikon DS - Fi2 was used to capture the images.

2.3. Statistical analysis

Whenever possible, experimental values of the various measures were subjected to statistical analysis, carried out by means of Astatsa statistical calculator; one-way analysis of variance (ANOVA) was followed by Scheffé post hoc comparisons ($p < 0.05$ was considered significant).

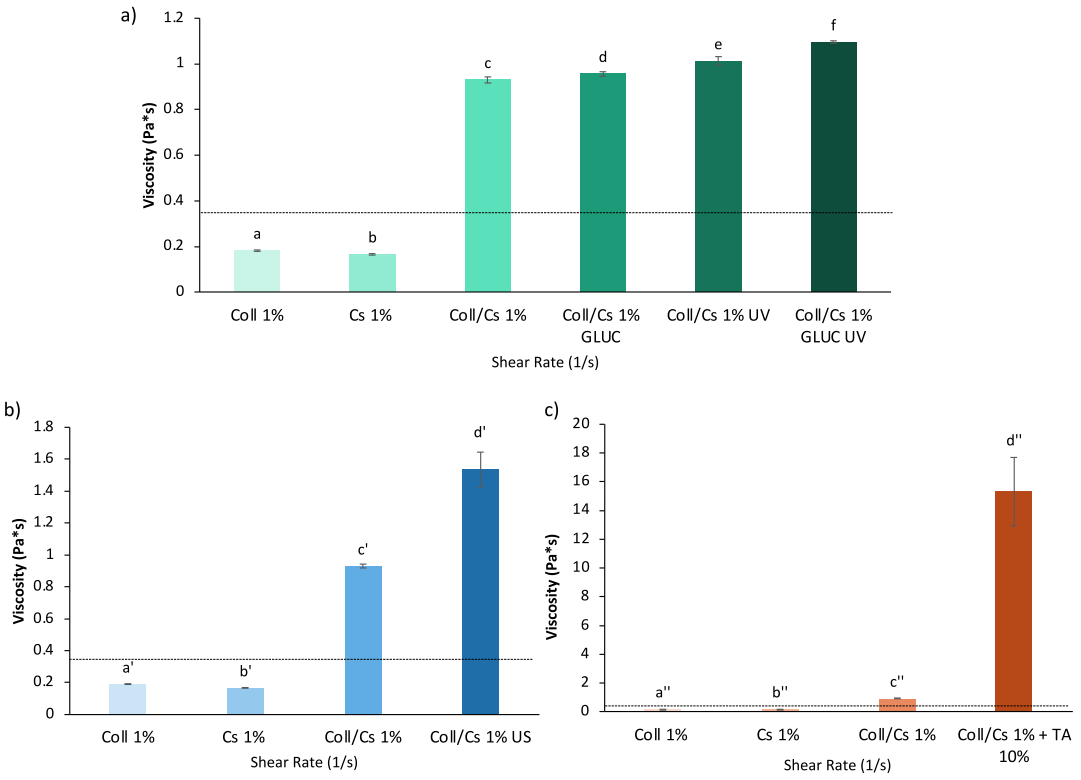

Fig. 1. Viscosity values (Pa*s) at 50 (s^{-1}) shear rate of a) Coll 1 %, Cs 1 % and Coll/Cs 1 % untreated or treated with GLUC, UV and GLU + UV; b) Coll 1 %, Cs 1 % and Coll/Cs 1 % untreated or treated with US; c) Coll 1 %, Cs 1 % and Coll/Cs 1 % untreated or treated with TA (mean values ± s.d.; $n = 3$). ANOVA one way; post hoc Scheffè test (p value ≤0.05): a vs b-f; b vs c-f; c vs e, f; d vs e, f.; e vs f; a′ vs b′-d′; b′ vs c′, d′; c′ vs d′; a″ vs b″-d″; b″ vs c″, d″; c″ vs d″.

3. Results and discussion

3.1. Hydrogels rheological properties

Cross-linking of Coll/Cs hydrogels is functional to obtain an insoluble matrix which does not dissolve in the biological fluids but undergoes a high swelling, in turn responsible for the diffusion of nutrients within the matrix. The formation of a 3D structure after swelling, like that of ECM, is particularly attracting for cells attachment and proliferation [34]. Among chemical cross-linking methods, UV irradiation and more in general photocross-linking, do not require any additional and potentially cytotoxic reagents, are easy to perform and environmentally friendly. The principal interaction of photoinitiators and compounds with light sensitivity creates free radicals interacting each other to obtain crosslinked hydrogels [27,30,35]. Ohan et al. [36], and later Davidenko et al. [30], proposed a method to increase the cross-linking degree of Coll-based scaffolds and to make them less susceptible to enzymatic degradation when compared to scaffolds obtained by UV treatment alone. Such method involves the incorporation of GLUC: the rapid generation of free radicals is promoted by the UV exposure, leading to the formation of GLUC-derived crosslinks which could react through glycosylation of the Coll structure, imparting strength and endurance to the scaffolds [30].

TA is a naturally occurring plant polyphenol, characterized by a central D-glucose molecule derivatized at its hydroxyl groups with one or more galloyl residues. Due to its phenolic groups, it can establish hydrogen bonds with different polymers and biological macromolecules, explaining its antioxidant capacity, hemostatic and antibacterial properties and making it suitable for the treatment of burns and wounds [37,38]. Sionkowska et al. demonstrated that TA is responsible for the cross-linking of a Coll/Cs mixture by forming hydrogen bonds with chemical moieties of Coll and Cs (one molecule of TA per one molecule of Coll and Cs, at the same time) thus providing highly porous hydrogels [37].

Ultrasonication (US) is another example of a physical cross-linking procedure, particularly useful to speed up the permanent sol-gel transition of different biomaterials. US is particularly interesting as cross-linking technique because it is recognized as an efficient, fast and green gelation process; moreover, this process is also compatible with fragile proteins, such as Coll, that can be easily denatured, for example at high temperatures [39]. US typically involves reactions that are improved using ultrasound radiation (20 kHz-10 MHz). In particular, at low-frequency radiation, hydrogen bonds and hydrophobic interactions are enhanced, while at higher frequency radiation polymerization reactions are supported, especially through the role of cavitation, which refers to nucleation, growth, oscillation and transient collapse of tiny gas or vapor bubbles caused from the internal pressure variation generated in the medium via ultrasound radiation [27]. The use of ultrasonication in hydrogels preparation leads to an increase of hydrogel stability and strength, without requiring chemical initiators while providing short reaction times and simple use, as well as a more uniform hydrogel structure [40]. Pok et al. demonstrated the feasibility of ultrasonication method in developing Cs-gelatin cross-linked freeze-dried hydrogels with 3D porous structure [32]. In the present work, Coll/Cs polymeric mixtures composed of 1 % *w*/w Coll and Cs were crosslinked with different methods (UV or GLUC + UV, TA and US) and after 24 h (gelation time) were subjected to viscosity measurements. It is well-known that the formation of cross-links produces an increase in polymer viscosity [41–43]. In order to evaluate the extent of cross-linking, the viscosity increment of the mixture upon cross-linking was investigated.

Fig. 1 reports viscosity mean values (Pa.s) measured at 50 s^{-1} for cross-linked Coll/Cs hydrogels: Coll/Cs 1 % *w*/w UV, Coll/CS 1 % + GLUC and Coll/Cs 1 % w/w + GLUC UV (Fig. 1a); Coll/Cs 1 % w/w US (Fig. 1b) and Coll/Cs 1 % w/w + TA 10 % (Fig. 1c). Coll 1 % w/w, Cs 1 % w/w (same concentrations as in the mixtures) solutions, and the

Table II
η_{mix}/η_t % values at 50 shear rates (s^{-1}) of all the Coll/Cs mixtures: Coll/Cs 1 %, Coll/Cs 1 % UV, Coll/Cs 1 % + GLU, Coll/Cs 1 % *w*/w + GLUC UV, Coll/Cs 1 % US, Coll/Cs 1 % w/w + TA 10 %. The untreated mixture Coll/Cs 1 % was considered as reference (mean values ± s.d.; n = 3). The theoretical value (sum of the viscosities of Coll 1 % and Cs 1 % solutions) correspond to 100 %. ANOVA one way; post hoc Scheffè test (p value ≤0.05): a vs b, d, e, f; b vs c- f; c vs d- f; d vs e, f; e vs f.

Sample	η_{mix}/η_t %
Theoretical value (Coll 1 % + Cs 1.0 %)	100
Coll/Cs 1 %	267 ± 5[a]
Coll/Cs 1 % UV	291 ± 8[b]
Coll/Cs 1 % + GLUC	274 ± 4[c]
Coll/Cs 1 % + GLUC UV	314 ± 2[d]
Coll/Cs 1 % US	440 ± 41[e]
Coll/Cs 1 % + TA 10 %	4398 ± 1188 [f]

untreated mixture (Coll/Cs) of the two polymers at 1 % w/w concentration, were used as references. It can be observed that the viscosity value of the untreated Coll/Cs mixture is higher than the sum of the viscosity values of the single polymeric solutions (theoretical value), indicating the occurrence of an interaction between the two polymers. Such an increase, named in literature as rheological synergism, has been extensively used to evaluate the interaction between mucoadhesive polymers and mucus glycoproteins [44–46]. It is generally accepted that chain interlocking and chemical interactions which occur between two polymers are likely to produce changes in the rheological behavior of the two macromolecular species. Positive rheological synergism values indicate the occurrence of such interactions.

It can be appreciated that all the treatments employed, except for the only addition of GLUC, lead to a significant increase in the viscosity value of the mixture (Fig. 1a, b, c). Moreover, Coll/Cs 1 % + GLUC UV is characterized by a viscosity value significantly higher than that of the mixture treated with UV only, indicating that the addition of GLUC can effectively enhance the UV cross-linking efficacy (Fig. 1a). The results

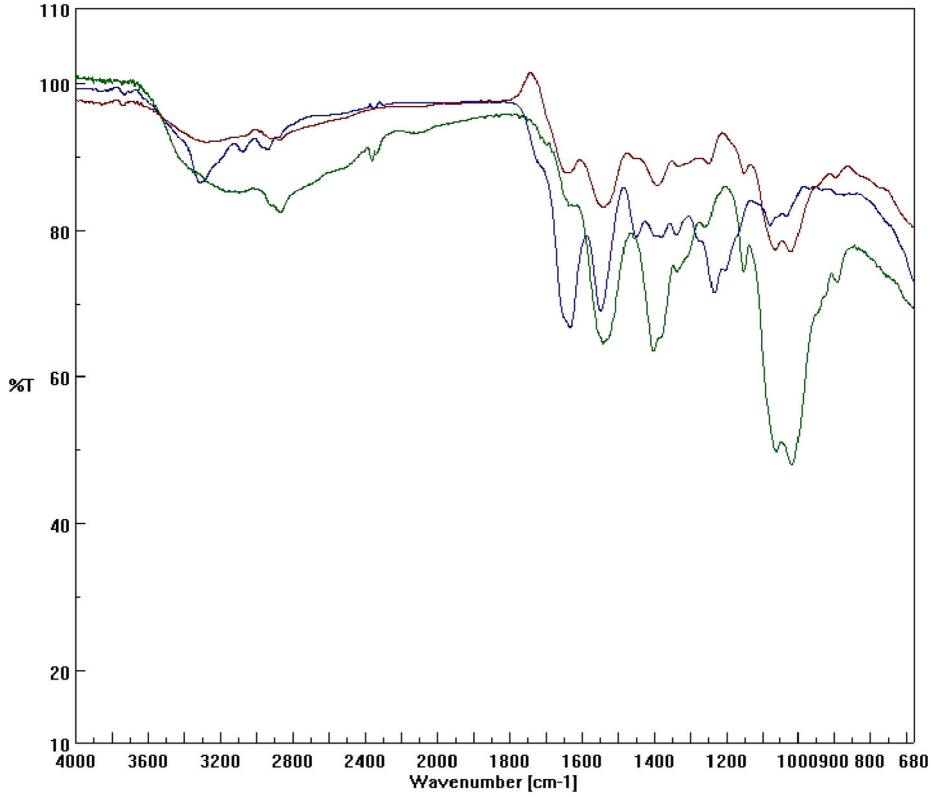

Fig. 2. FTIR spectra of Coll 1 % (blue profile), Cs 1 % (green profile) and Coll/Cs 1 % mixture (red profile).

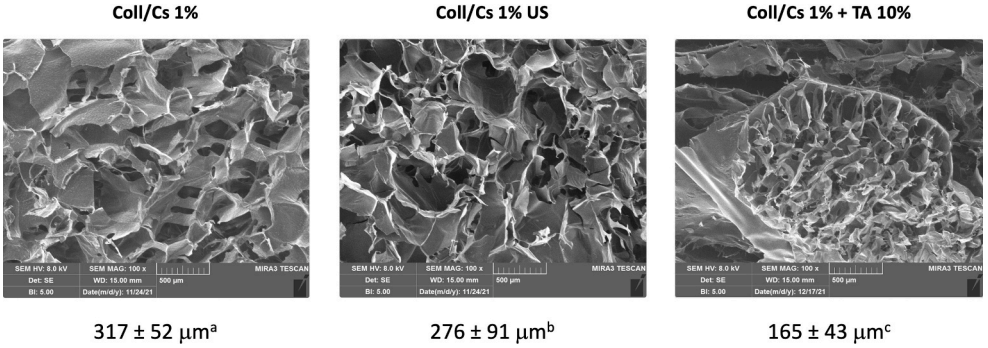

Fig. 3. SEM images of Coll/Cs 1 %, Coll/Cs 1 % US and Coll/Cs 1 % + TA 10 %. Pore size of each specimen is also reported. Pore size evaluation was performed with ImageJTM software (mean values ± sd; *n* = 30) ANOVA one way; post hoc Scheffè test (*p* value ≤0.05): a vs b-c; b vs c.

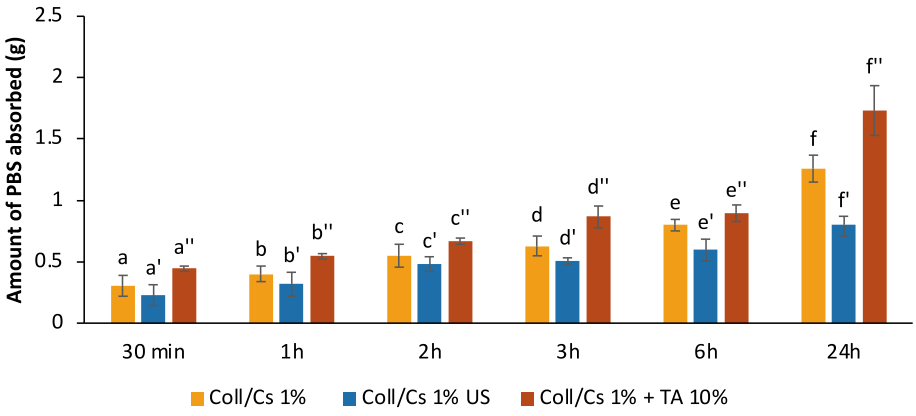

Fig. 4. Amount of PBS absorbed by Coll/Cs 1 %, Coll/Cs 1 % US and Coll/Cs 1 % + TA 10 % as a function of time (30 min, 1 h, 2 h, 3 h, 6 h, 24 h) (mean values ± sd; $n = 3$) ANOVA one way; post hoc Scheffè test (p value ≤0.05): a vs a″; a′ vs a″; b vs b″; b′ vs b″; c′ vs c″; d vs d′, d″; d′ vs d″; e vs e′; e′ vs e″; f vs f′, f″; f′ vs f″.

Table III
Swelling ratio values of freeze-dried hydrogels Coll/Cs 1 %, Coll/Cs 1 % US and Coll/Cs 1 % + TA 10 % (mean values ± s.d.; $n = 3$). ANOVA one way; post hoc Scheffè test (p value ≤0.05): a vs b, c; b vs c.

Sample	Swelling ratio
Coll/Cs 1 %	36.5 ± 0.8^{a}
Coll/Cs 1 % US	25.6 ± 0.6^{b}
Coll/Cs 1 % + TA 10 %	40.8 ± 0.4^{c}

obtained confirm the efficacy of all the cross-linking techniques employed. Viscosity variation % (η_{mix}/η_t %) was calculated in order to establish the best cross-linking methods in terms of viscosity increment [44–46].

In Table II are reported the η_{mix}/η_t % values for the hydrogels treated with the different cross-linking methods. The value of 100 % corresponds to the theoretical value calculated as the sum of Coll 1 % *w*/w and Cs 1 % w/w viscosities. The simple mixing of the two polymers (Coll/Cs 1 %) produces a viscosity value more than twice the theoretical value (dotted line in the figures), indicating the occurrence of interactions between the two polymers. Among the cross-linking techniques considered, TA shows the highest value of the viscosity variation %, followed by US. It must be underlined that for Coll/Cs 1 % + TA 10 %, such parameter is characterized by a very high variability, that could be index of a poor sample homogeneity. On the basis of the obtained results, Coll/Cs 1 % US and Coll/Cs + TA 10 %, which are the samples characterized by the highest viscosity values, were chosen for the prosecution of the work.

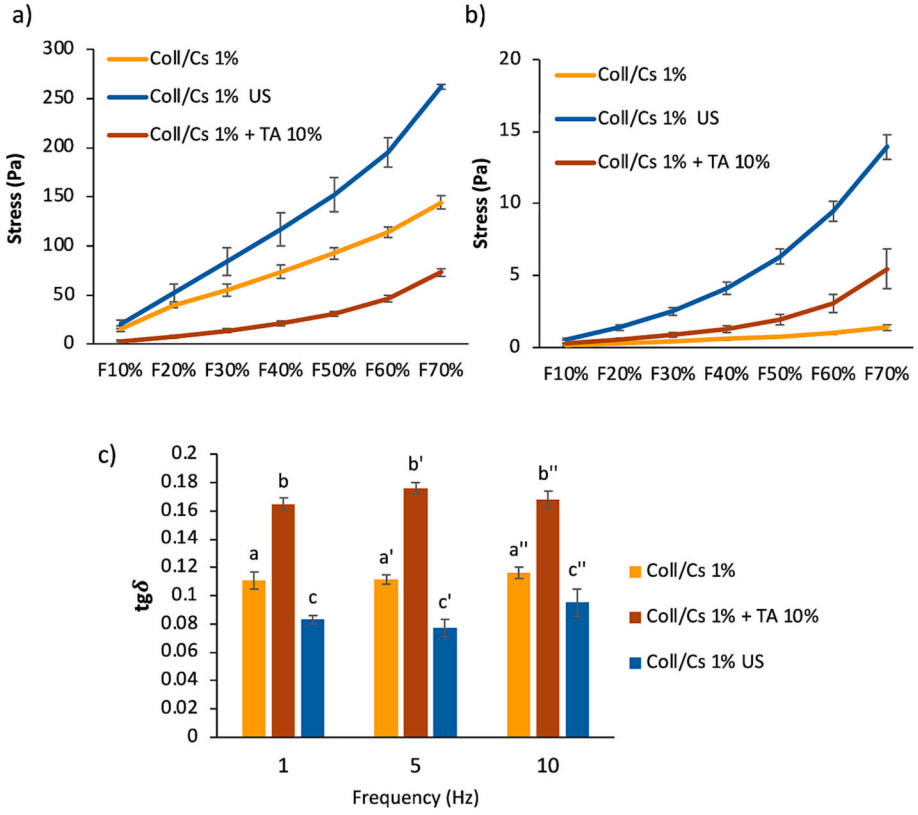

Fig. 5. a) Stress-strain profiles of the freeze-dried hydrogels Coll/Cs 1 %, Coll/Cs 1 % + TA 10 % and Coll/Cs 1 % US (mean values ± s.d.; $n = 3$); b) stress-strain profiles of hydrated freeze-dried Coll/Cs 1 %, Coll/Cs 1 % + TA 10 % and Coll/Cs 1 % US (mean values ± s.d.; n = 3); c) loss tangent (tang δ) of Coll/Cs 1 %, Coll/Cs 1 % + TA 10 % and Coll/Cs 1 % US (mean values ± s.d.; n = 3). ANOVA one way; post hoc Scheffè test (p value ≤0.05): a vs b, c; b vs c; a′ vs b′, c′; b′ vs c′; a″ vs b″, c″; b″ vs c″.

Table IV
Compression work values (AUC. N·mm) of freeze-dried Coll/Cs 1 %, Coll/Cs 1 % + TA 10 % and Coll/Cs 1 % US as such and upon hydration in PBS (mean values ± s.d.; n = 3) ANOVA one way; post hoc Scheffè test (p value ≤0.05).

Sample	AUC (N·mm)	
	Dried	Hydrated
Coll/Cs 1.0 %	7,673 ± 538	0.29 ± 0.02
Coll/Cs 1.0 % US	12,041 ± 700	2.42 ± 0.21
Coll/Cs 1.0 % + TA 10 %	2,554 ± 217	1.27 ± 0.25

Table V
Stress (Pa) and compression work (AUC (N·mm)) of freeze-dried Coll/Cs US DoE samples (mean values ± s.d.; $n = 3$). ANOVA one way; post hoc Scheffè test (p value ≤0.05): Stress: a vs b- i; b vs c, e, f, g, h, i; c vs d- i; d vs e- i; e vs f- i; f vs g, i; g vs h, i; h vs i. AUC: a′ vs b′-i′; b′ vs c′-i′; c′ vs d′, e′, f′, g′, h′, i′; d′ vs e′-i′; e′ vs f′-i′; f′ vs g′, i′; g′ vs h′, i′; h′ vs i′.

Sample	Stress (Pa)	AUC (N·mm)
Coll/Cs 1	12 ± 3^{a}	$4.9 \pm 0.6^{a'}$
Coll/Cs 2	35.6 ± 0.8^{b}	$20 \pm 3^{b'}$
Coll/Cs 3	71 ± 6^{c}	$43 \pm 3^{c'}$
Coll/Cs 4	45 ± 9^{d}	$28 \pm 7^{d'}$
Coll/Cs 5	97.8 ± 0.8^{e}	$55 \pm 2^{e'}$
Coll/Cs 6	224 ± 34^{f}	$130 \pm 30^{f'}$
Coll/7 s 7	121 ± 2^{g}	$71.2 \pm 0.9^{g'}$
Coll/Cs 8	216 ± 4^{h}	$118 \pm 4^{h'}$
Coll/Cs 9	311 ± 31^{i}	$179 \pm 16^{i'}$

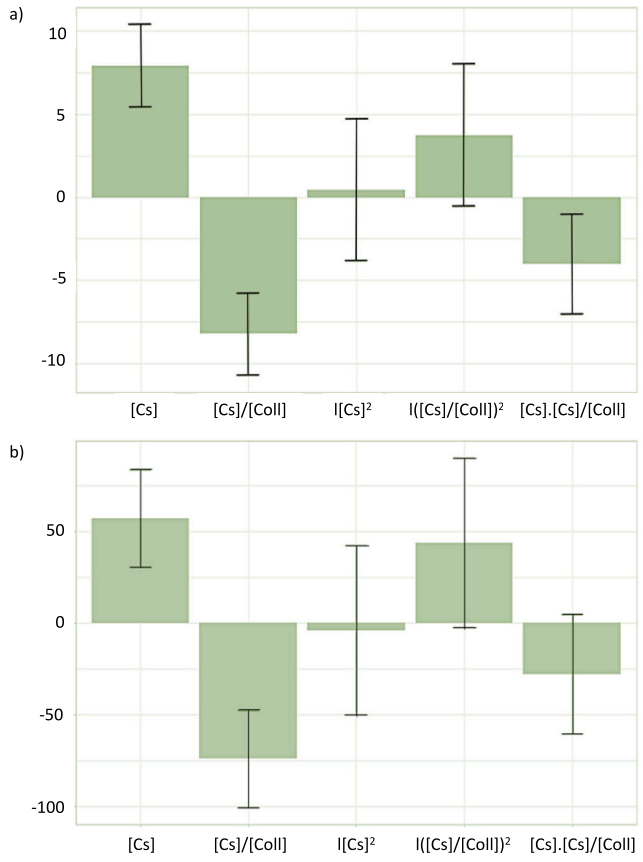

Fig. 6. a) Bar plot representing the factor coefficient magnitude and the associated error bar, at the 95 % confidence interval, for the response variable Stress (Pa); b) bar plot representing the factor coefficient magnitude and the associated error bar, at the 95 % confidence interval, for the response variable compression work (N·mm). R^2 of both models resulted to be >0.9.

3.2. FTIR analysis

Fig. 2 shows the FTIR spectra of pure Cs, pure Coll, and Coll/Cs 1 % mixture. The spectrum of Cs displays, among others, the characteristics peaks of amide I around 1590 cm^{-1} (N—H group bending) and of the –OH vibrations around 1400 cm^{-1}. Other intense peaks are observed around 1100–900 cm^{-1} and are ascribed to the glycosidic bonds [47]. The FTIR spectrum of Coll presents the typical amide I, II and III bands around 1640, 1550 and 1230 cm^{-1}. The spectrum of the hydrogel composed by a 1:1 mixture of Coll and Cs displays, essentially, the most intense band of the constituent materials, without the appearance of notable additional peaks. This behavior has been observed in other cross-linked CS/Coll systems where the interaction occurs mainly by hydrogen bonds formation between the -OH, $-NH_2$ and -C=O groups in Coll with -OH and $-NH_2$ in Cs [48]. Further indication of the formation of an interaction between the two compounds comes from a general reduction of intensity of the amide groups of Coll suggesting the participation of the amino groups in the bonding formation [49].

3.3. Freeze-dried hydrogels characterization

After freeze-drying process, morphological, hydration and mechanical properties of Coll/Cs hydrogels cross-linked by US and TA were evaluated. The freeze-dried untreated mixture was considered as reference.

3.3.1. Morphological properties

Fig. 3 reports the SEM images of all the three samples. Their morphological 3D porous interconnected structures can be appreciated. In particular, the mixture treated with TA shows a drastic reduction in pore size and a less organized structure when compared to the untreated sample. On the other hand, Coll/Cs US sample is characterized by a more regular structure with a less marked variation in pore size with respect to the untreated sample. This result is in line with previous reports indicating US is a suitable method to enhance the stability and strength of the hydrogel by providing a uniform inner structure [40].

3.3.2. Hydration properties

Values of PBS amount absorbed during time from the three different scaffolds are reported in Fig. 4. As can be observed, untreated scaffold, together with the one cross-linked by US, are characterized by not statistically different values of the amount of PBS absorbed up to 2 h. After 3 h hydration, Coll/Cs 1 % displayed higher values of PBS absorbed with respect to the ultrasonicated one, probably as a consequence of an increased looseness of the structure deriving from the lack of a cross-linking treatment. On the contrary, the scaffold cross-linked with TA is characterized by the highest profile of buffer absorbed. Table III reports swelling ratio values calculated on the untreated freeze-dried hydrogel compared with the ones cross-linked with US and TA, respectively, upon 24 h hydration in pH 7.4 PBS medium. It can be observed that Coll/Cs 1 % + TA 10 % is the specimen characterized by the highest swelling ratio value, significantly higher with respect to that of the untreated sample. This could be explained by the presence of TA contributing to the increase of the number of hydrophilic groups present in the scaffold, improving the final scaffold hydrophilicity and thus the capability to interact with water [50]. Instead, Coll/Cs 1 % US showed the lowest value of swelling ratio, probably because US enhances the occurring of hydrophilic interactions between Coll and Cs, subtracting hydrophilic groups of Coll and Cs from the interaction with water [32].

3.3.3. Mechanical properties: compression stress, work of compression and viscoelastic behavior

Freeze-dried samples (Coll/Cs 1 %, Coll/Cs 1 % US, Coll/Cs 1 % + TA 10 %), as such and upon hydration in PBS for 24 h at 37 °C, were subjected to a compression test to evaluate their mechanical properties before and after their application into the wound bed. PBS was chosen as

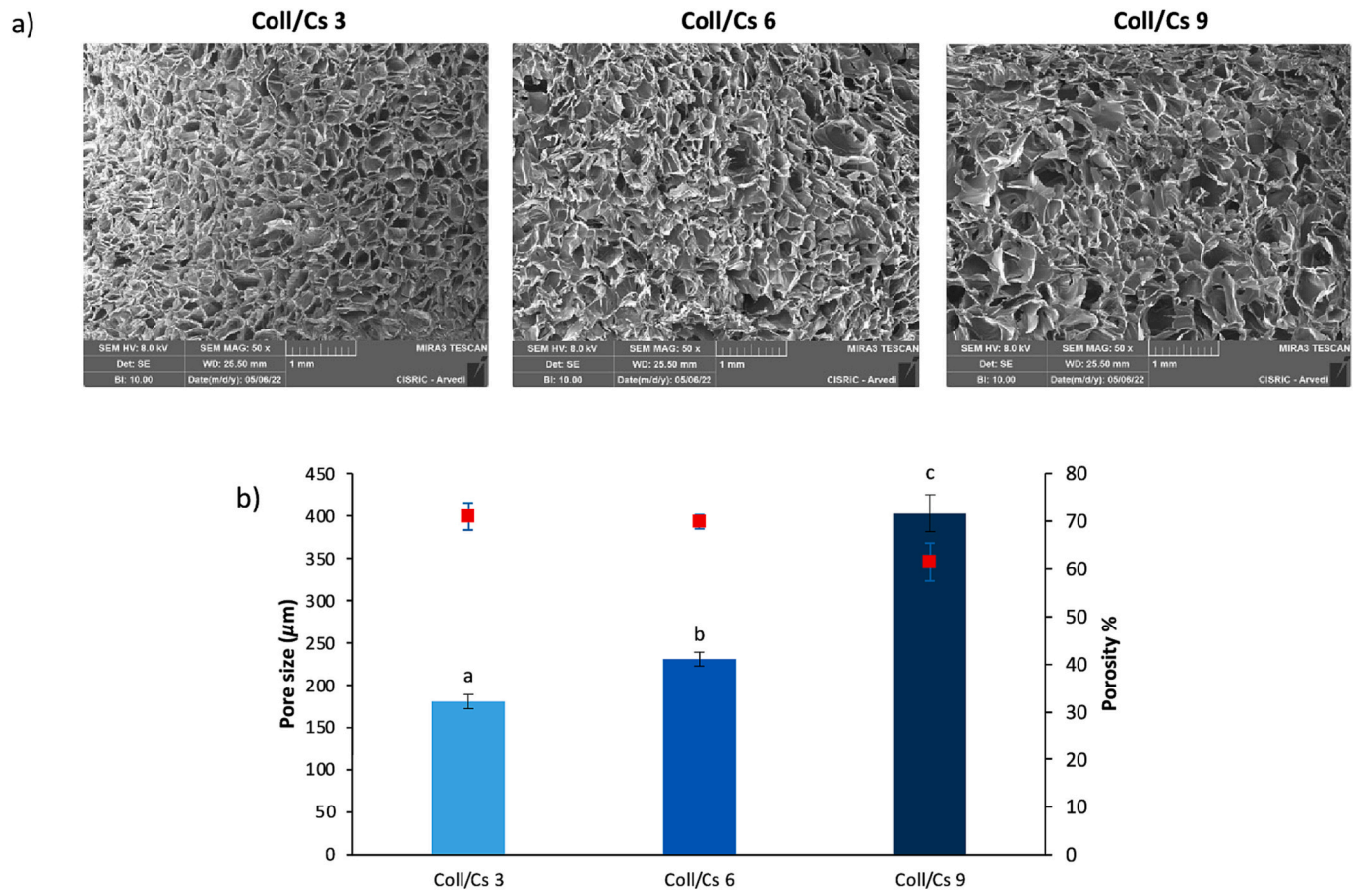

Fig. 7. a) SEM images of Coll/Cs 3, Coll/Cs 6 and Coll/Cs 9, at 50× of magnification; b) histogram: mean pore size (μm) of Coll/Cs 3, Coll/Cs 6 and Coll/Cs 9. Pore size evaluation with ImageJTM software (mean values ± sd; $n = 30$) ANOVA one way; post hoc Scheffè test (p value ≤0.05): a vs b-c; b vs c; squares: mean porosity (P %) values of Coll/Cs 3, Coll/Cs 6 and Coll/Cs 9 (mean values ± s.d.; n = 3) ANOVA one way; post hoc Scheffè test (p value ≤0.05): a vs b-c; b vs c.

Table VI
Swelling ratio values of US freeze-dried hydrogels Coll/Cs 3, Coll/Cs 6 and Coll/Cs 9 (mean values ± s.d.; $n = 3$). ANOVA one way; post hoc Scheffè test (p value ≤0.05): c vs a, b.

Sample	Swelling ratio
Coll/Cs 3	20.4 ± 3.0^{a}
Coll/Cs 6	21.4 ± 1.4^{b}
Coll/Cs 9	14.4 ± 0.8^{c}

medium mimicking the wound exudate. Upon application into the wound bed, the freeze-dried matrix should absorb the wound exudate thanks to its hydrophilicity and porosity, forming a gel made insoluble by cross-links. Fig. 5a and b shows stress vs strain profiles of the freeze-dried and hydrated samples, respectively. In Table IV are reported the compression work values for all the samples considered. As expected, all the samples, upon hydration, resulted to be softer and deformable, a behavior suitable for in vivo application.

Coll/Cs 1 % US is characterized by the highest stress-strain profiles and by the greatest values of compression work in both dry and hydrated state. A different behavior is observed for Coll/Cs 1 % + TA 10 % depending on its hydration state. While the dry sample is characterized by a higher stress-strain profile and a greater compression work value with respect to the untreated mixture, upon hydration the performance of the two products reverses; when hydrated, the sample offering a major resistance to penetration is the untreated mixture. This behavior can be explained by the different sample hydration tendency as suggested by the swelling ratio parameter (see Section 3.3.2). Indeed, US cross-linked Coll/Cs was the sample characterized by the lowest swelling behavior, meaning that it absorbs a lower PBS amount compared to the other two samples. Oppositely, when put in contact with PBS, TA cross-linked sample is characterized by the highest value of swelling ratio. The higher hydration of the sample is responsible for the decrease resistance penetration, that results to be even lower than that observed for the untreated mixture.

Furthermore, viscoelastic measurements were performed on hydrated samples and the corresponding loss tangent (tang δ) values for Coll/Cs 1 %, Coll/Cs 1 % + TA 10 % and Coll/Cs 1 % US were calculated (Fig. 5c). It can be observed that all the three samples are characterized by a prevalence of the elastic behavior on the viscous one as indicated by tang δ values (calculates as G''/G' ratio) lower than 1. The viscoelastic properties of the samples are in line with those of the compression test performed on hydrated samples. Coll/Cs 1 % US shows the lowest tang δ value, which increases moving to Coll/Cs 1 % and Coll/Cs 1 % + TA 10 %. Therefore, sample cross-linked by US is characterized by the highest elastic contribution.

Moreover, the viscoelastic behavior of the three scaffolds is in accordance with their hydration properties: Coll/Cs 1 % US is characterized by the lowest maximum PBS amount absorbed and swelling ratio at 24 h, followed in increasing order, by Coll/Cs 1 % and by Coll/Cs 1 % + TA 10 % (Fig. 4). The PBS amount absorbed is responsible for the polymeric network hydration impacting on its ability to elastically react under the application of a stress. Minor is the PBS absorbed, higher is the system elasticity.

According to the results of compression test and viscoelastic measurements, US was identified as the best cross-linking method for Coll/Cs hydrogels due to its capability in forming a matrix with the best

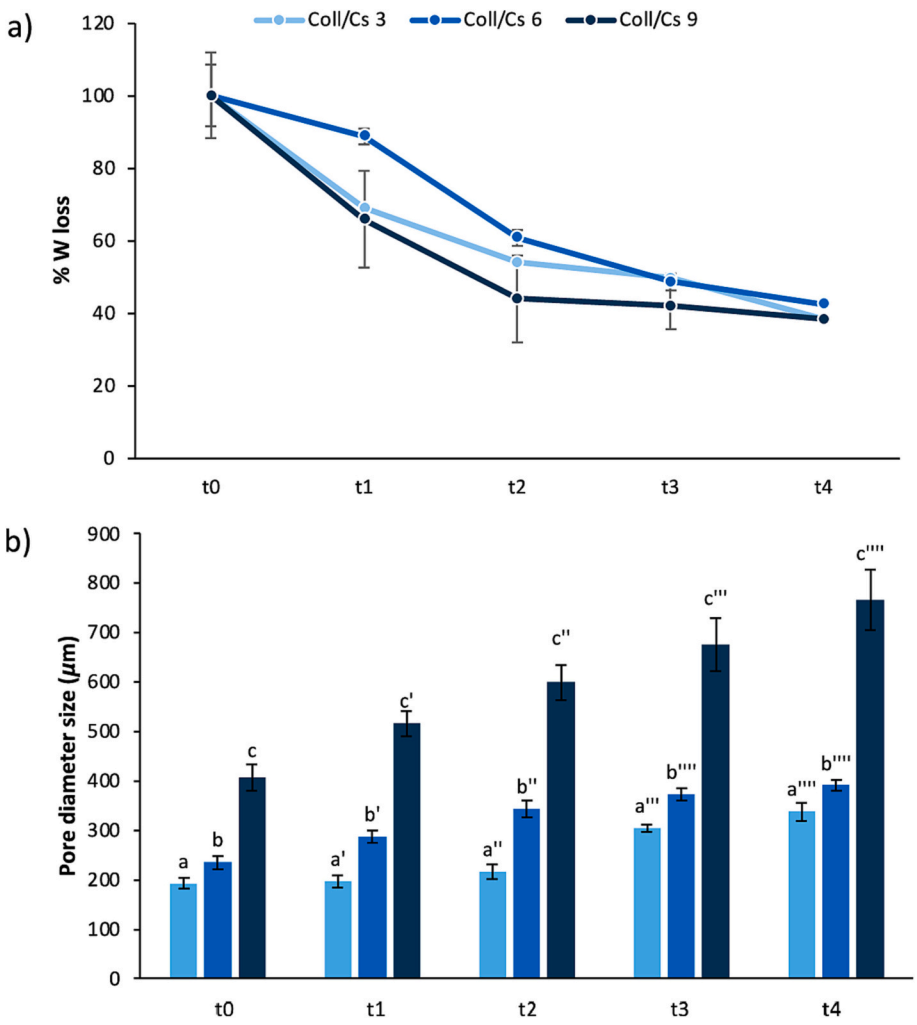

Fig. 8. a) % loss on dry weight (%W) calculated for each sample at different time points: t0 (0 days), t1 (7days), t2 (14 days), t3 (21days), t4 (28days) (mean values ± sd; $n = 30$); b) pore diameter size (μm) of Coll/Cs 3, Coll/Cs 6 and Coll/Cs 9 subjected to degradation test for 28 days. Size evaluation performed with ImageJTM software (mean values ± sd; n = 30). ANOVA one way; post hoc Scheffè test (p value ≤0.05): a vs b, c; b vs c; a′ vs b′, c′; b′ vs c′; a″ vs b″, c″; b″ vs c″; a‴ vs b‴, c‴; b‴ vs c‴; a⁗ vs b⁗, c⁗; b⁗ vs c⁗.

mechanical and elastic properties. Such properties are responsible for the ability of the scaffold to properly withstand external stresses possibly present during in vivo implantation [51].

3.4. Influence of US freeze-dried sample composition on mechanical properties: DoE approach

Once ultrasonication was defined as the best cross-linking method, additional studies were focused on the identification of the most suitable Coll/Cs hydrogel composition, varying the concentration and the ratio between Coll and Cs.

In detail, a DoE approach was performed in order to evaluate, on statistical basis, the influence of Cs concentration [Cs] and of the concentration ratio between Cs and Coll, [Cs]/[Coll], on the mechanical properties of the sample. A "full factorial design" 3^k (k = 2) containing all possible combinations between the factors, i.e. [Cs] and [Cs]/[Coll], and their levels (high (+), medium (0) and low (−)) was chosen. Nine freeze-dried Coll/Cs matrices (see experimental part, Section 2.2.5) were prepared and characterized to test the mechanical properties. Maximum stress (Pa) and compression work (AUC (N•mm)) were considered as the response variables. Table V reports the results of the 9 samples considered. It can be observed that among samples 3, 5, 7, containing an equal total polymer concentration (1.5 %), sample 7, prepared with the highest Cs concentration, is characterized by the best mechanical properties. As expected, samples 3, 6 and 9, characterized by the highest total polymer concentration, show the highest value of both the two response variables.

Fig. 6a and b shows the coefficients bar plots for the response variables considered; magnitude, sign and confidential level are reported. It can be noted that [Cs]/[Coll] is the factor with the greatest influence on both the parameters maximum stress and compression work; in particular, [Cs]/[Coll] has a statistically negative effect on both stress and compression work, meaning that mechanical properties improve when such factor decreases. [CS] has a statistically significative positive effect on both the response variables, meaning that the mechanical properties are better on increasing Cs concentration.

Coll/Cs 3, Coll/Cs 6 and Coll/Cs 9 prepared from CS solutions at 0.5, 0.75 and 1 %, respectively, were chosen for the prosecution of the work. The weight ratio between CS and Coll for all the solutions was equal to 0.5.

3.5. US Freeze-dried hydrogel characterization

3.5.1. Morphological properties

Fig. 7a and b displays the SEM images and pore size of US freeze-dried Coll/CS hydrogels (samples 3, 6 and 9). It can be observed that an increase in the total amount of polymers lead to a less organized internal structure, without regular pore distribution and dimensions. The most organized structure is that of Coll/Cs 3, characterized by the lowest Cs and Coll concentrations. Fig. 7b reports the pore size (histogram) and porosity % (squared points). According to the results, the US freeze-dried hydrogel with the smallest pore size was Coll/Cs 3 (0.5 % Cs, 1 % Coll). Regarding porosity % values, as expected, Coll/Cs 3 (0.5 % Cs, 1 % Coll) and Coll/Cs 6 (0.75 % Cs, 1 % Coll) are characterized by the

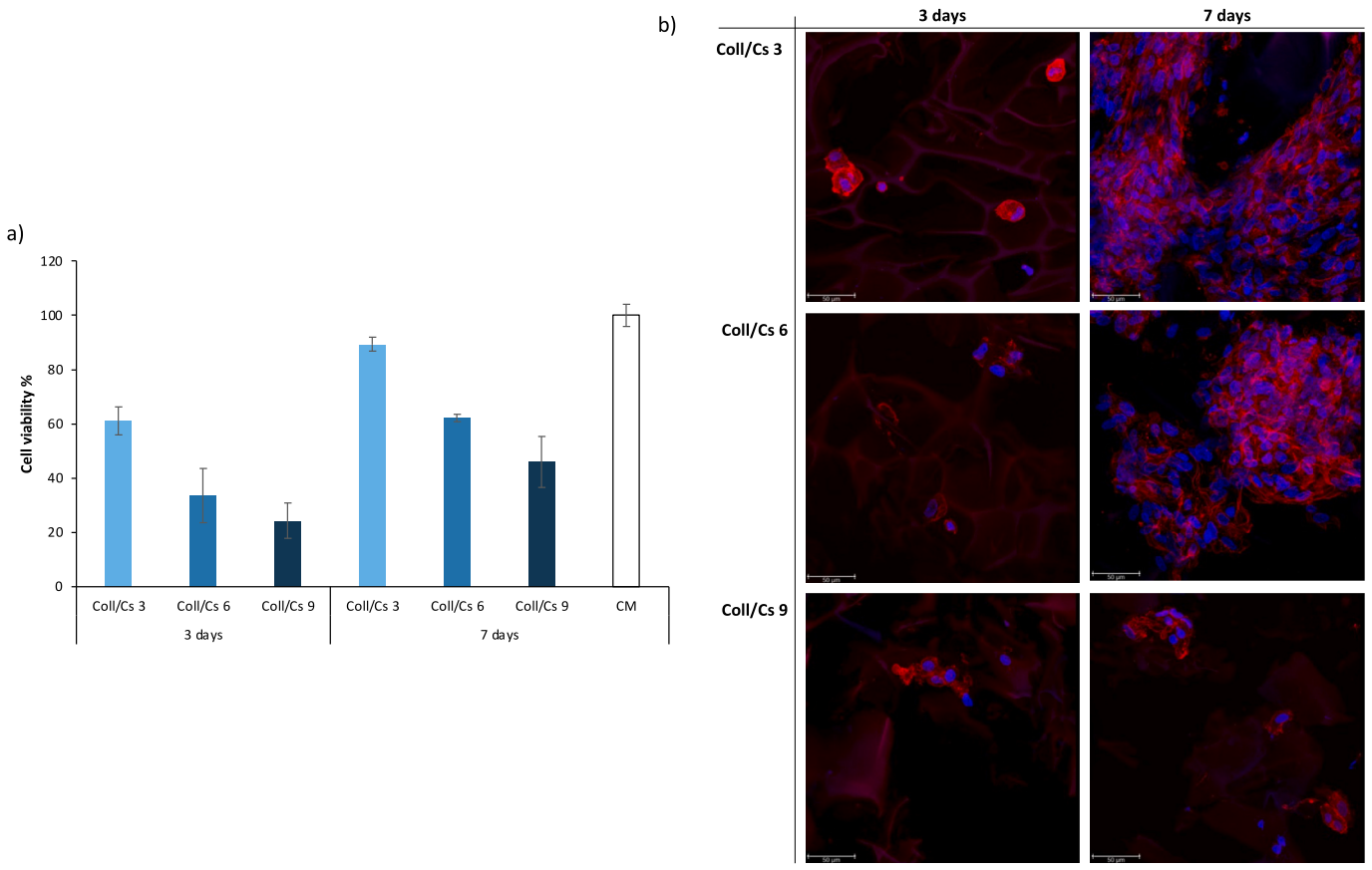

Fig. 9. a) Viability % values calculated after 7 days of cells contact with Coll/Cs 3, Coll/Cs 6 and Coll/Cs 9 (mean values ± s.d.; $n = 6$). CM was considered as control. ANOVA one-way; post hoc Scheffè test ($p < 0.05$): Coll/Cs 6 at 3 days vs Coll/Cs 9 at 3 days; b) CLSM Microphotographs of NHDF grown on Coll/Cs 3, Coll/Cs 6 and Coll/Cs 9, for 3 and 7 days: confocal-laser scanning microscopy; nuclei in blue, Hoechst 33258; cytoskeleton in red, TRITC. Scale bars: 50 μm.

highest mean P% values, which are statistically different from that of Coll/Cs 9 (1 % Cs, 2 % Coll): increasing polymer concentrations corresponds to a decrease in sample porosity%.

3.5.2. Hydration properties

Table VI lists the swelling ratio values, calculated on the three US freeze-dried scaffolds upon 24 h hydration in pH 7.4 PBS medium. All the samples can absorb a high PBS amount, since all the calculated swelling ratios are in the range from 14.4 ± 0.8 to 21.4 ± 3.0. This means that the samples can absorb PBS reaching weight values up to ≈ 15 − 20 times their initial weight. After in vivo application at the site of injury, the highly porous structure of these samples allows the absorption and the drainage of the wound exudate, with the consequent formation of a gel, resembling the hydrated ECM microenvironment thus creating an ideal architectural pattern in which cells can proliferate [52].

Notably, a different hydration is observed depending on the amount of Coll and Cs present in the scaffold. As a matter of fact, Coll/Cs 3 and Coll/Cs 6 are characterized by higher swelling ratio values if compared to Coll/Cs 9. These results could be explained considering that higher concentrations of the two polymers lead to the formation of an excessively interconnected network that hinders the hydration process of the scaffold. The porosity % results previously shown can support this statement since the Coll/Cs 9 was the sample characterized by the lowest porosity % value.

3.5.3. In vitro degradation properties

A degradation test was performed on US freeze-dried hydrogels Coll/Cs 3, Coll/Cs 6 and Coll/Cs 9 to evaluate scaffolds stability in PBS medium at 37 °C for 28 days. Fig. 8a shows the comparison between % loss on dry weight (%W) of each sample at different time points: t0 (0 days), t1(7 days), t2 (14 days), t3 (21 days), t4 (28 days), calculated as reported in Section 2.2.6.4. All the three scaffolds do not reach values below 40 % of W% after 28 days of immersion in PBS medium.

Morphologic properties of the scaffolds were also evaluated at each time point by measuring the pore size (μm) of the US freeze-dried hydrogels (Coll/Cs 3, Coll/Cs 6 and Coll/Cs 9) after soaking in PBS. The results are reported in Fig. 8b and show an increase in pore size by increasing time due to the greater laxity of the structure caused by the degradation of the scaffold with time.

3.5.4. In vitro cell proliferation and adhesion properties

The cell proliferation and adhesion properties of the optimized US cross-linked Coll/Cs freeze-dried hydrogels were assessed on NHDF. NHDF cells represent one of the most suitable model cell lines for in vitro evaluation of scaffolds intended for the treatment of skin injuries, as they are the most abundant cell type in all connective tissues and play an important role in wound healing process [53,54].

Results of the proliferation test are reported in Fig. 9a as the percentage of living cells after contact with the freeze-dried hydrogels after 3 and 7 days. After 3 days of contact, all the samples show low cell viability % values. It could depend on the fact that cells need time to enter the scaffold architecture and to contact each other. After 7 days, Coll/Cs 3 sample was characterized by a marked increment of % cell viability, higher with respect to the other samples, confirming the proliferation enhancement of such scaffold. Moreover, Fig. 9b shows CLSM microphotographs of NHDF grown on freeze-dried hydrogels, after 3 and 7 days, during cell adhesion assay. It is evident that cell proliferation on Coll/Cs 9 was limited when compared to Coll/Cs 3 and Coll/Cs 6. In fact, Coll/Cs 3 and Coll/Cs 6 microphotographs reveal that the cells

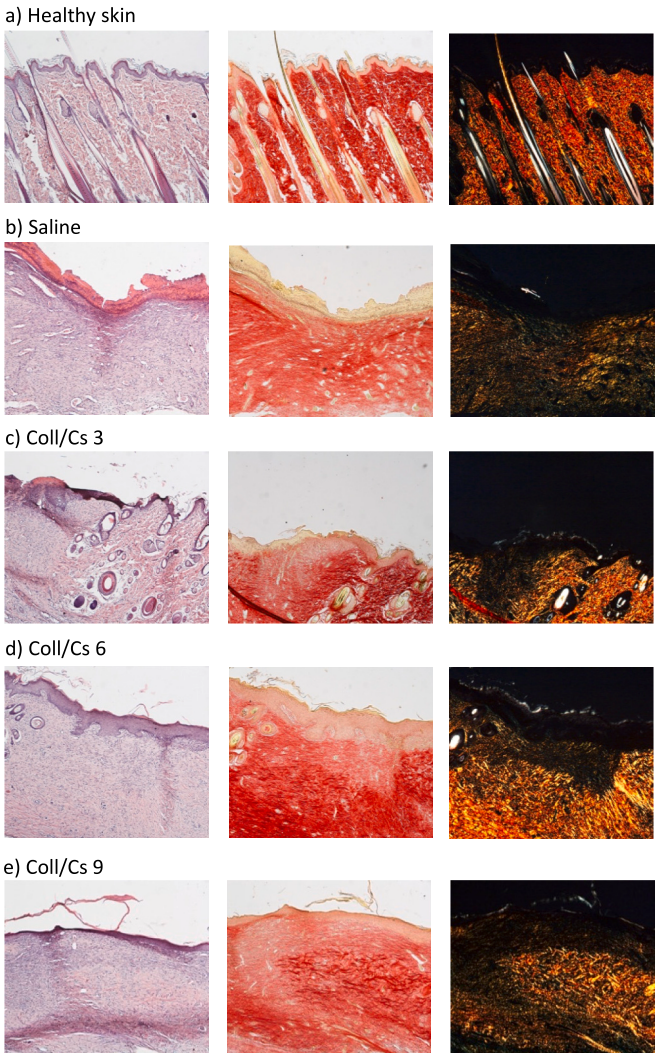

Fig. 10. H&E (upper panel) and PSR (lower panel - with bright field images; right panel - with polarized light) sections of (a) intact skin, (b) lesion treated with saline solution as negative control, (c), (d) and (e) lesion treated with the three different Coll/CS scaffolds. Original magnification: Original magnification: 5×. Each micrograph frame has a width of 1780 μm.

proliferated and grown on and inside the porous 3D interconnected scaffold, resulting in a complete colonization. In particular, Coll/Cs 3 showed the highest extent of cell colonization. It is clear from both the tests performed that Coll/Cs 3 has a superior ability in supporting and facilitating cell adhesion and growth, suggesting an optimal cells-substrate interaction, probably due to the fact that it is characterized by a lower total amount of polymers with respect to the other two samples, that in turn is responsible, as mentioned above, for the lowest pore size (about 170 μm), 70 % porosity, and a high swelling ratio. These are all key factors to create a suitable environment for cell attachment and growth.

3.5.5. In vivo wound healing properties (rat model)

Results of in vivo biocompatibility are reported in Fig. 10. After 18-day treatment, for each sample, the wound area was totally reconstituted with a completely regenerated epithelium. The treatment with saline solution (control) resulted in a less advanced healing stage with respect to the treatments with the three scaffolds.

All the treated samples still showed signs of the proliferative phase of healing, with several forming blood vessels and a residual area of granulation tissue (a mixture of proliferating capillaries, fibroblast and inflammatory cells in a loose edematous extracellular matrix). In particular, it was observed an increase in granulation tissue as the total amount of Coll and Cs increases. According to that, sample treated with Coll/Cs 3 was characterized by the lowest amount of granulation tissue (extension area of <1 mm) meaning that it was the sample at the most advanced stage of healing process, if compared with the others two. However, the entire surface of the lesion treated with the freeze-dried hydrogels was covered with new epithelium, fully restored in multiple layers of cells and with a fair degree of keratinization. Skin appendages, such as hair follicles and glands, were reforming. Collagen was laid down and remodeled in an appropriate orientation to withstand the tensile stresses placed on the repair area, suggesting a maturation and remodeling phase of the healing process [55–57]. Moreover, PSR stain showed a continuous collagen layer, rich in orange-to-red fibers, with a pattern identical to that of intact skin, confirming the complete safety of the scaffolds. These results indicate that US Coll/Cs freeze-dried hydrogels can be used as effective wound dressings as they ensure a regular healing process while providing effective protection from infections for the presence of Cs [22]. Especially, Coll/Cs 3 resulted to be the most promising one, confirming in vitro experiments results. After 18-day treatment, no scaffold or part of it was observed, indicating a complete biodegradation. This result suggests that the Coll/Cs scaffold is characterized by an in vivo degradation process that is suitable for the complete regeneration and healing of the wounds. The fact that the scaffold degradation goes along, in terms of time, with the healing process, is a desirable property for wound medications. Moreover, no sign of local inflammation was observed at the site of the implant. Therefore, the ability of the degrading scaffold to provide wound healing, without triggering an immune response, could suggest that the Coll/Cs based scaffolds herein developed could be promising dressings for chronic skin injuries.

Both Cs and Coll are recognized to be strictly involved in wound healing process promotion. Fibroblast activation, migration and proliferation, cytokine production, stimulation of the synthesis of Coll type IV and polymorphonuclear cell activation are among Cs principal biochemical activities in wound healing [58]. Coll is a mediator of various key steps that are critical for a successful wound healing process, namely inflammation, angiogenesis, formation of the granulation tissue, re-epithelization, and platelet aggregation [59]. Because of the commitment of Cs and Coll in regulation and modulation of such processes, a hydrogel wound dressing composed of them could be highly promising for the promotion of wound healing process.

4. Conclusions

A promising biodegradable cross-linked porous scaffold consisting of Coll and Cs was developed for the treatment of chronic skin ulcers. Three different cross-linking methods were investigated to identify the most suitable one for Coll and Cs. As a result, the ultrasonication method was found to be the ideal cross-linking method due to its ability in providing a hydrogel with the best compromise between mechanical properties and elastic behavior. Furthermore, a DoE approach was successfully employed to investigate the influence of Cs concentration (% *w*/w) and Cs and Coll weight ratio on ultrasonicated cross-linked scaffold mechanical properties. In vitro studies on a model cell line (Fibroblast cells) pointed out the best performance of the Cs/Coll 3 scaffold in promoting cell proliferation and adhesion. The best regenerative potential of such scaffold was confirmed in a murine model.

Further work on the Cs/Coll manufacturing process is planned in order to obtain a scaffold with standardized structural properties. In addition, a deeper evaluation of the consistency of the structure throughout the scaffold and from one scaffold to another needs to be performed [60]. The final prototype obtained should be subjected to a further characterization such as hemocompatibility and systemic toxicity, important criteria for their successful in vivo applicability [61,62].

CRediT authorship contribution statement

Caterina Valentino: Conceptualization, Formal analysis, Investigation, Methodology, Resources, Writing – original draft, Writing – review & editing. **Barbara Vigani:** Data curation, Formal analysis, Investigation, Methodology, Resources. **Gaia Zucca:** Formal analysis, Investigation, Writing – original draft. **Marco Ruggeri:** Data curation, Investigation. **Cinzia Boselli:** Data curation, Formal analysis, Investigation. **Antonia Icaro Cornaglia:** Investigation. **Lorenzo Malavasi:** Data curation, Formal analysis, Writing – review & editing. **Giuseppina Sandri:** Data curation, Funding acquisition, Methodology. **Silvia Rossi:** Conceptualization, Funding acquisition, Methodology, Project administration, Supervision, Writing – review & editing.

Declaration of competing interest

The authors declare that they have no known competing financial interests or personal relationships that could have appeared to influence the work reported in this paper.

Acknowledgements

The authors would like to thank Dr. Alessandro Girella (CISRiC Arvedi, University of Pavia) for his assistance in SEM analyses.

References

[1] K. las Heras, M. Igartua, E. Santos-Vizcaino, R.M. Hernandez, Chronic wounds: current status, available strategies and emerging therapeutic solutions, J. Control. Release 328 (2020) 532–550, https://doi.org/10.1016/j.jconrel.2020.09.039.
[2] M. Ruggeri, E. Bianchi, S. Rossi, B. Vigani, M.C. Bonferoni, C. Caramella, G. Sandri, F. Ferrari, Nanotechnology-based medical devices for the treatment of chronic skin lesions: from research to the clinic, Pharmaceutics. 12 (2020) 1–32, https://doi.org/10.3390/pharmaceutics12090815.
[3] D. Simões, S.P. Miguel, M.P. Ribeiro, P. Coutinho, A.G. Mendonça, I.J. Correia, Recent advances on antimicrobial wound dressing: a review, Eur. J. Pharm. Biopharm. 127 (2018) 130–141, https://doi.org/10.1016/j.ejpb.2018.02.022.
[4] M. Mirhaj, S. Labbaf, M. Tavakoli, A.M. Seifalian, Emerging treatment strategies in wound care, Int. Wound J. 19 (2022) 1934–1954, https://doi.org/10.1111/iwj.13786.
[5] M. Liang, Z. Chen, F. Wang, L. Liu, R. Wei, M. Zhang, Preparation of self-regulating/anti-adhesive hydrogels and their ability to promote healing in burn wounds, J Biomed Mater Res B Appl Biomater 107 (2019) 1471–1482, https://doi.org/10.1002/jbm.b.34239.
[6] K.R. Hixon, R.C. Klein, C.T. Eberlin, H.R. Linder, W.J. Ona, H. Gonzalez, S.A. Sell, A critical review and perspective of honey in tissue engineering and clinical wound healing, Adv. Wound Care (New Rochelle). 8 (2019) 403–415, https://doi.org/10.1089/wound.2018.0848.
[7] S.P. Miguel, A.F. Moreira, I.J. Correia, Chitosan based-asymmetric membranes for wound healing: a review, Int. J. Biol. Macromol. 127 (2019) 460–475, https://doi.org/10.1016/j.ijbiomac.2019.01.072.
[8] K. Varaprasad, T. Jayaramudu, V. Kanikireddy, C. Toro, E.R. Sadiku, Alginate-based composite materials for wound dressing application: a mini review, Carbohydr. Polym. 236 (2020), https://doi.org/10.1016/j.carbpol.2020.116025.
[9] A. Ahmed, G. Getti, J. Boateng, Ciprofloxacin-loaded calcium alginate wafers prepared by freeze-drying technique for potential healing of chronic diabetic foot ulcers, Drug Deliv. Transl. Res. 8 (2018) 1751–1768, https://doi.org/10.1007/s13346-017-0445-9.
[10] Y. Fan, M. Lüchow, Y. Zhang, J. Lin, L. Fortuin, S. Mohanty, A. Brauner, M. Malkoch, Nanogel encapsulated hydrogels as advanced wound dressings for the controlled delivery of antibiotics, Adv. Funct. Mater. 31 (2021), https://doi.org/10.1002/adfm.202006453.
[11] S. Mantha, S. Pillai, P. Khayambashi, A. Upadhyay, Y. Zhang, O. Tao, H.M. Pham, S.D. Tran, Smart hydrogels in tissue engineering and regenerative medicine, Materials. 12 (2019), https://doi.org/10.3390/ma12203323.
[12] M. Farokhi, M. Aleemardani, A. Solouk, H. Mirzadeh, A.H. Teuschl, H. Redl, Crosslinking strategies for silk fibroin hydrogels: promising biomedical materials, Biomed. Mater. (Bristol). 16 (2021), https://doi.org/10.1088/1748-605X/abb615.
[13] N. Poorgholy, B. Massoumi, M. Ghorbani, M. Jaymand, H. Hamishehkar, Intelligent anticancer drug delivery performances of two poly(N-isopropylacrylamide)-based magnetite nanohydrogels, Drug Dev. Ind. Pharm. 44 (2018) 1254–1261, https://doi.org/10.1080/03639045.2018.1442845.
[14] M. Abbasian, B. Massoumi, R. Mohammad-Rezaei, H. Samadian, M. Jaymand, Scaffolding polymeric biomaterials: are naturally occurring biological macromolecules more appropriate for tissue engineering? Int. J. Biol. Macromol. 134 (2019) 673–694, https://doi.org/10.1016/j.ijbiomac.2019.04.197.
[15] C. Fan, D.A. Wang, Macroporous hydrogel scaffolds for three-dimensional cell culture and tissue engineering, Tissue Eng. Part B Rev. 23 (2017) 451–461, https://doi.org/10.1089/ten.teb.2016.0465.
[16] C.R. Carvalho, R.L. Reis, J.M. Oliveira, Fundamentals and current strategies for peripheral nerve repair and regeneration, in: Adv Exp Med Biol, Springer, 2020, pp. 173–201, https://doi.org/10.1007/978-981-15-3258-0_12.
[17] N. Asadi, A.R. del Bakhshayesh, S. Davaran, A. Akbarzadeh, Common biocompatible polymeric materials for tissue engineering and regenerative medicine, Mater. Chem. Phys. 242 (2020), https://doi.org/10.1016/j.matchemphys.2019.122528.
[18] S. Pina, J.M. Oliveira, R.L. Reis, Natural-based nanocomposites for bone tissue engineering and regenerative medicine: a review, Adv. Mater. 27 (2015) 1143–1169, https://doi.org/10.1002/adma.201403354.
[19] C.R. Carvalho, R.L. Reis, J.M. Oliveira, Fundamentals and current strategies for peripheral nerve repair and regeneration, in: Adv Exp Med Biol, Springer, 2020, pp. 173–201, https://doi.org/10.1007/978-981-15-3258-0_12.
[20] F. Copes, N. Pien, S. van Vlierberghe, F. Boccafoschi, D. Mantovani, Collagen-based tissue engineering strategies for vascular medicine, Front. Bioeng. Biotechnol. 7 (2019), https://doi.org/10.3389/fbioe.2019.00166.
[21] C. Dong, Y. Lv, Application of collagen scaffold in tissue engineering: recent advances and new perspectives, Polymers (Basel). 8 (2016), https://doi.org/10.3390/polym8020042.
[22] M.M. Islam, M. Shahruzzaman, S. Biswas, M. Nurus Sakib, T.U. Rashid, Chitosan based bioactive materials in tissue engineering applications-a review, Bioact. Mater. 5 (2020) 164–183, https://doi.org/10.1016/j.bioactmat.2020.01.012.
[23] I. Aranaz, A.R. Alcántara, M.C. Civera, C. Arias, B. Elorza, A.H. Caballero, N. Acosta, Chitosan: an overview of its properties and applications, Polymers (Basel) 13 (2021), https://doi.org/10.3390/polym13193256.
[24] A. Martínez, M.D. Blanco, N. Davidenko, R.E. Cameron, Tailoring chitosan/collagen scaffolds for tissue engineering: effect of composition and different crosslinking agents on scaffold properties, Carbohydr. Polym. 132 (2015) 606–619, https://doi.org/10.1016/j.carbpol.2015.06.084.
[25] A. Anitha, S. Sowmya, P.T.S. Kumar, S. Deepthi, K.P. Chennazhi, H. Ehrlich, M. Tsurkan, R. Jayakumar, Chitin and chitosan in selected biomedical applications, Prog. Polym. Sci. 39 (2014) 1644–1667, https://doi.org/10.1016/j.progpolymsci.2014.02.008.
[26] M. Rodríguez-Vázquez, B. Vega-Ruiz, R. Ramos-Zúñiga, D.A. Saldaña-Koppel, L. F. Quiñones-Olvera, Chitosan and its potential use as a scaffold for tissue engineering in regenerative medicine, Biomed. Res. Int. 2015 (2015), https://doi.org/10.1155/2015/821279.
[27] M. Farokhi, M. Aleemardani, A. Solouk, H. Mirzadeh, A.H. Teuschl, H. Redl, Crosslinking strategies for silk fibroin hydrogels: promising biomedical materials, Biomed. Mater. (Bristol) 16 (2021), https://doi.org/10.1088/1748-605X/abb615.
[28] Q.L. Loh, C. Choong, Three-dimensional scaffolds for tissue engineering applications: role of porosity and pore size, Tissue Eng. Part B Rev. 19 (2013) 485–502, https://doi.org/10.1089/ten.teb.2012.0437.
[29] S. Vijayavenkataraman, Nerve guide conduits for peripheral nerve injury repair: a review on design, materials and fabrication methods, Acta Biomater. 106 (2020) 54–69, https://doi.org/10.1016/j.actbio.2020.02.003.
[30] N. Davidenko, D.v. Bax, C.F. Schuster, R.W. Farndale, S.W. Hamaia, S.M. Best, R. E. Cameron, Optimisation of UV irradiation as a binding site conserving method for crosslinking collagen-based scaffolds, J. Mater. Sci. Mater. Med. 27 (2016) 1–17, https://doi.org/10.1007/s10856-015-5627-8.
[31] A. Sionkowska, B. Kaczmarek, K. Lewandowska, Modification of collagen and chitosan mixtures by the addition of tannic acid, J. Mol. Liq. 199 (2014) 318–323, https://doi.org/10.1016/j.molliq.2014.09.028.
[32] S. Pok, J.D. Myers, S.v. Madihally, J.G. Jacot, A multilayered scaffold of a chitosan and gelatin hydrogel supported by a PCL core for cardiac tissue engineering, Acta Biomater. 9 (2013) 5630–5642, https://doi.org/10.1016/j.actbio.2012.10.032.
[33] S. Zeng, L. Liu, Y. Shi, J. Qiu, W. Fang, M. Rong, Z. Guo, W. Gao, Characterization of silk fibroin/chitosan 3D porous scaffold and in vitro cytology, PLoS One 10 (2015), https://doi.org/10.1371/journal.pone.0128658.
[34] M. Rahmati, D.K. Mills, A.M. Urbanska, M.R. Saeb, J.R. Venugopal, S. Ramakrishna, M. Mozafari, Electrospinning for tissue engineering applications, Prog. Mater. Sci. 117 (2021), https://doi.org/10.1016/j.pmatsci.2020.100721.
[35] K. Adamiak, A. Sionkowska, Current methods of collagen cross-linking: review, Int. J. Biol. Macromol. 161 (2020) 550–560, https://doi.org/10.1016/j.ijbiomac.2020.06.075.
[36] S. Anastase-Ravion, M.P. Carreno, C. Blondin, O. Ravion, J. Champion, F. Chaubet, N. Haeffner-Cavaillon, D. Letourneur, Synergistic effects of glucose and ultraviolet irradiation on the physical properties of collagen, J. Biomed. Mater. Res. 60 (2002) 384–391, https://doi.org/10.1002/jbm.10111.
[37] A. Sionkowska, B. Kaczmarek, K. Lewandowska, Modification of collagen and chitosan mixtures by the addition of tannic acid, J. Mol. Liq. 199 (2014) 318–323, https://doi.org/10.1016/j.molliq.2014.09.028.
[38] S. Rivero, M.A. García, A. Pinotti, Crosslinking capacity of tannic acid in plasticized chitosan films, Carbohydr. Polym. 82 (2010) 270–276, https://doi.org/10.1016/j.carbpol.2010.04.048.
[39] W. Xiao, W. Liu, J. Sun, X. Dan, D. Wei, H. Fan, Ultrasonication and genipin cross-linking to prepare novel silk fibroin-gelatin composite hydrogel, J. Bioact. Compat. Polym. 27 (2012) 327–341, https://doi.org/10.1177/0883911512448692.
[40] K. Liu, L. Yan, R. Li, Z. Song, J. Ding, B. Liu, X. Chen, 3D printed personalized nerve guide conduits for precision repair of peripheral nerve defects, Adv. Sci. 9 (2022), https://doi.org/10.1002/advs.202103875.

[41] N. Shah, R.K. Mewada, T. Mehta, Crosslinking of starch and its effect on viscosity behaviour, Rev. Chem. Eng. 32 (2016) 265–270, https://doi.org/10.1515/revce-2015-0047.
[42] K.S. Sandhu, A.K. Siroha, S. Punia, L. Sangwan, M. Nehra, S.S. Purewal, Effect of degree of cross linking on physicochemical, rheological and morphological properties of Sorghum starch, Carbohydr. Polym. Technol. Appl. 2 (2021), https://doi.org/10.1016/j.carpta.2021.100073.
[43] M.C. Montoya-Ospina, H. Verhoogt, T.A. Osswald, Processing and rheological behavior of cross-linked polyethylene containing disulfide bonds, SPE Polym. 3 (2022) 25–40, https://doi.org/10.1002/pls2.10062.
[44] B. Vigani, C. Valentino, G. Sandri, C.M. Caramella, F. Ferrari, S. Rossi, Spermidine crosslinked gellan gum-based "hydrogel nanofibers" as potential tool for the treatment of nervous tissue injuries: a formulation study, Int. J. Nanomedicine 17 (2022) 3421–3439, https://doi.org/10.2147/IJN.S368960.
[45] S. Rossi, B. Vigani, M.C. Bonferoni, G. Sandri, C. Caramella, F. Ferrari, Rheological analysis and mucoadhesion: a 30 year-old and still active combination, J. Pharm. Biomed. Anal. 156 (2018) 232–238, https://doi.org/10.1016/j.jpba.2018.04.041.
[46] S. Mouftah, M.M.A. Abdel-Mottaleb, A. Lamprecht, Buccal delivery of low molecular weight heparin by cationic polymethacrylate nanoparticles, Int. J. Pharm. 515 (2016) 565–574, https://doi.org/10.1016/j.ijpharm.2016.10.039.
[47] C. Lustriane, F.M. Dwivany, V. Suendo, M. Reza, Effect of chitosan and chitosan-nanoparticles on post harvest quality of banana fruits, J. Plant Biotechnol. 45 (2018) 36–44, https://doi.org/10.5010/JPB.2018.45.1.036.
[48] L.L. Fernandes, C.X. Resende, D.S. Tavares, G.A. Soares, L.O. Castro, J.M. Granjeiro, Cytocompatibility of Chitosan and Collagen-Chitosan Scaffolds for Tissue Engineering, n.d.
[49] X. Ma, J. Deng, Y. Du, X. Li, D. Fan, C. Zhu, J. Hui, P. Ma, W. Xue, A novel chitosan-collagen-based hydrogel for use as a dermal filler: initial in vitro and in vivo investigations, J. Mater. Chem. B 2 (2014) 2749–2763, https://doi.org/10.1039/c3tb21842b.
[50] W. Yan, M. Shi, C. Dong, L. Liu, C. Gao, Applications of tannic acid in membrane technologies: a review, Adv. Colloid Interf. Sci. 284 (2020), https://doi.org/10.1016/j.cis.2020.102267.
[51] A. Giménez, J.J. Uriarte, J. Vieyra, D. Navajas, J. Alcaraz, Elastic properties of hydrogels and decellularized tissue sections used in mechanobiology studies probed by atomic force microscopy, Microsc. Res. Tech. 80 (2017) 85–96, https://doi.org/10.1002/jemt.22740.
[52] X. Zhang, M. Qin, M. Xu, F. Miao, C. Merzougui, X. Zhang, Y. Wei, W. Chen, D. Huang, The fabrication of antibacterial hydrogels for wound healing, Eur. Polym. J. 146 (2021), https://doi.org/10.1016/j.eurpolymj.2021.110268.
[53] G. Sriram, P.L. Bigliardi, M. Bigliardi-Qi, Fibroblast heterogeneity and its implications for engineering organotypic skin models in vitro, Eur. J. Cell Biol. 94 (2015) 483–512, https://doi.org/10.1016/j.ejcb.2015.08.001.
[54] A. el Ghalbzouri, P. Hensbergen, S. Gibbs, J. Kempenaar, R. van der Schors, M. Ponec, Fibroblasts facilitate re-epithelialization in wounded human skin equivalents, Lab. Investig. 84 (2004) 102–112, https://doi.org/10.1038/labinvest.3700014.
[55] A.J. Singer, R.A.F. Clark, Cutaneous Wound Healing 341, 1999, pp. 738–746, https://doi.org/10.1056/NEJM199909023411006.
[56] M.M. Agwa, S. Sabra, N.A. Atwa, H.A. Dahdooh, R.M. Lithy, H. Elmotasem, Potential of frankincense essential oil-loaded whey protein nanoparticles embedded in frankincense resin as a wound healing film based on green technology, J. Drug Deliv. Sci. Technol. 71 (2022), 103291, https://doi.org/10.1016/J.JDDST.2022.103291.
[57] A.A. Hemmati, A. Larki-Harchegani, S. Shabib, A. Jalali, A. Rezaei, G. Housmand, Wound healing property of milk in full thickness wound model of rabbit, Int. J. Surg. 54 (2018) 133–140, https://doi.org/10.1016/J.IJSU.2018.04.030.
[58] R. Singh, K. Shitiz, A. Singh, Chitin and chitosan: biopolymers for wound management, Int. Wound J. 14 (2017) 1276–1289, https://doi.org/10.1111/M.iwj.12797.
[59] S.S. Mathew-Steiner, S. Roy, C.K. Sen, Collagen in wound healing, Bioengineering. 8 (2021), https://doi.org/10.3390/bioengineering8050063.
[60] A. Campos Marin, D. Lacroix, The inter-sample structural variability of regular tissue-engineered scaffolds significantly affects the micromechanical local cell environment, Interface Focus 5 (2) (2015) 20140097, https://doi.org/10.1098/rsfs.2014.0097.
[61] M. Weber, H. Steinle, S. Golombek, L. Hann, C. Schlensak, W.P. Wendel, Avci-Adali blood-contacting biomaterials: in vitro evaluation of the hemocompatibility, Front. Bioeng. Biotechnol. 6 (2018) 99, https://doi.org/10.3389/fbioe.2018.00099.
[62] J.F. Kirk, G. Ritter, I. Finger, D. Sankar, J.D. Reddy, J.D. Talton, C. Nataraj, S. Narisawa, J.L. Millán, R.R. Cobb, Mechanical and biocompatible characterization of a cross-linked collagen-hyaluronic acid wound dressing, Biomatter 3 (4) (2013), e25633, https://doi.org/10.4161/biom.25633.